

ULTIMATE-Subaru: Sensitivity Estimates

Sadman Ali, Yusei Koyama, Kentaro Motohara, Yosuke Minowa,
Yoshito Ono, Ichi Tanaka

December 2, 2023

1 Introduction

The ULTIMATE-Subaru project aims to develop a wide field adaptive optics (GLAO) and a wide field near-infrared imaging camera (WFI) for the Subaru telescope. The goal will be to deploy the two systems in conjunction at the Cassegrain focus, such that the GLAO wavefront sensor will feed in turbulence corrected NIR light to the WFI, allowing for a science field of view of 14 x 14 square arcmin and excellent image quality/sensitivity. This in turn will facilitate large scale survey programs to be conducted in the NIR, particularly aimed at studying the formation and evolution of galaxies, among other key areas of research.

This document will summarise the current sensitivity estimates for the WFI+GLAO system and the key parameters used in the calculations. The sensitivity calculator is also available for use by science teams.

2 Background Models

The sensitivity is strongly dependent on both the sky background noise in the NIR as well as the thermal background noise from the non-cryogenic telescope mirrors/instruments, the latter of which starts to dominate the tail-end of the NIR (particularly in the K-band). As such the models adopted for both is of significant importance to the calculation of accurate sensitivities.

2.1 Sky background

For the sky background we adopt the Gemini IR models for Mauna Kea, particularly from 9000Å to 25000Å. The models are made up of a continuum, with the NIR emission lines (mostly very narrow OH lines) superimposed on top. The continuum consists of a zodiacal component which is approximated as a 5800K blackbody, and a thermal component which is treated as a 273K blackbody based on the temperature at Mauna Kea, both scaled by the atmospheric transmission. The background models are available for a number of airmasses (1.0, 1.5, 2.0) and water vapor columns (1.0mm, 1.6mm, 3.0mm, 5.0mm).

It should be noted that the strength of the OH lines can vary significantly throughout the night on a timescale of < 15 minutes and amplitudes up to 10%. As such the sensitivities are inherently

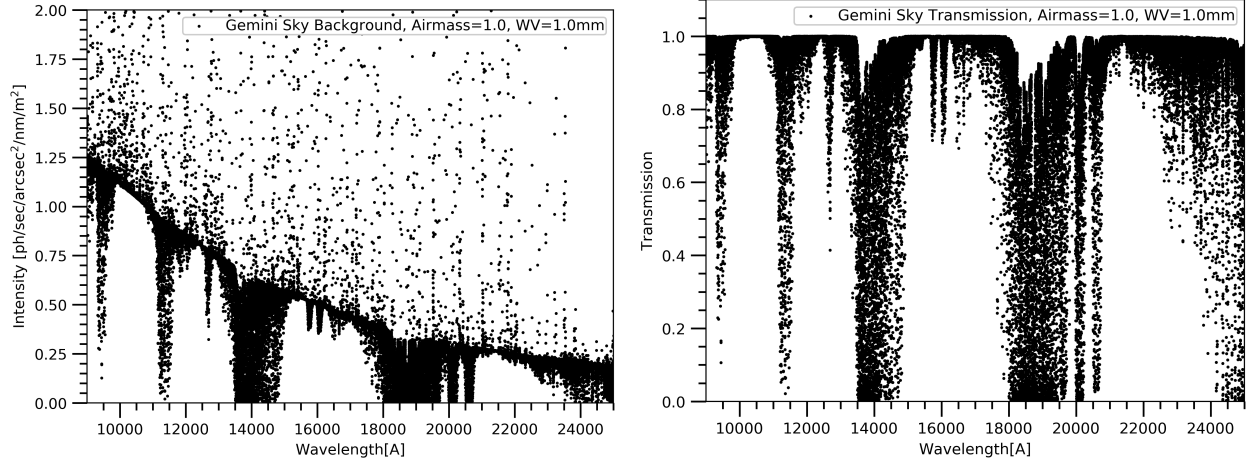


Figure 1: *Left:* Gemini sky background model for Mauna Kea. *Right:* Gemini Sky Transmission Model. Both models assume an airmass of 1.0 and a water vapor column of 1.0mm.

affected by this uncertainty, particularly in narrow-band filters. For our calculations we adopt the best case model with airmass of 1.0 and water vapor of 1.0mm. Fig 1 shosw the sky background model and the atmospheric transmission spectrum for the aforementioned airmass and water vapor column.

2.2 Telescope background

At the Cassegrain focus we have to take into account the thermal emission from the telescope's primary and secondary mirrors, upstream from the cryogenic NIR instrument. The telescope black-body emission is modelled by the following equation:

$$I_{tel} = \Omega_t \Lambda^2 \int \frac{2c}{\lambda^4(e^{hc/kT_{tel}\lambda}) - 1} \eta_i d\lambda, \quad (1)$$

where I_{tel} is in $\text{photons/sec/arcsec}^2$, η_i is the total throughput of the science instrument (including filter and quantum efficiency), T_{tel} is the temperature of the mirrors - assumed to be 273K, Λ is the physical size of the focal plane that corresponds to 1 arcsec on the sky and Ω_t is the emissivity-weighted solid angle as given by the following equation:

$$\Omega_t = \frac{\pi}{4f^2} [\{\epsilon_{m2} + \epsilon_{m1}(1 - \epsilon_{m2})\}(1 - v_c^2) + \epsilon_c^2 v_c^2], \quad (2)$$

where f is the telescope's effective focal ratio - 12.4 at the Cassegrain focus, ϵ_{m1} and ϵ_{m2} are the emissivities of the primary and secondary mirrors (defined as 1-reflectivity), v_c is the fraction of the central obscuration by the central cone on the telescope secondary mirror (~ 28), and ϵ_c is the emissivity of the center cone surface (~ 0.02).

2.3 Moon background

The emission from the moon, while mostly affecting the optical wavelengths, can still contribute to the shorter wavelength end of the NIR. As such we incorporated a model of the moon background

from Jones et al. (2019), who note the continuum emission of the moonlight to the overall observed night spectrum using X-Shooter out to the K-band. Generally the moonlight mostly contributes to the Y-band and to a small degree the J-band, but is negligible in the H and K-bands. Additionally, Roth et al. (2016) using sky observations using Gemini at Mauna Kea that the moon distance and moon phase has very little effect on the sky brightness in the NIR, with a small correlation found at very small moon distances to the Y-band sky brightness.

2.4 Readout Noise

While the read noise is generally negligible for broad/medium-band observations and long exposure times, it can become a considerable fraction of the overall noise in the case of narrow-band observations and/or very short exposure times (i.e. a few seconds). As such we adopt $16\text{ e}^-/\text{RMS}$ value for the readout noise for the H4RG WFI detector.

3 SENSITIVITY PARAMETERS

Sensitivities are calculated for a point source with the assumption that for long exposures the photon contribution from the object is negligible compared to the various sources of background noise. The following are the key parameters used in the calculation.

3.1 50% Encircled Energy (GLAO & NOAO)

One of the key benefits of the implementation of a GLAO system is a significant improvement in the image quality over having no adaptive optics (NOAO) capability. In our calculations the image quality is represented by the 50% encircled energy (EE_{50}) diameter of the Point Spread Function (PSF) in GLAO vs NOAO cases. The final PSF observed is a convolution of the GLAO corrected PSF with the science instrument PSF, the former of which has been determined by GLAO performance simulation and optimisation of the system specifications. The EE_{50} diameter was then determined from the final PSF at increasing wavelength intervals at different seeing conditions - good (25%), moderate (50%) and bad (75%). The EE_{50} diameter and FWHM values are shown in Table 1. In all cases GLAO provides a smaller EE_{50} diameter compared to NOAO, as would be expected. The sensitivity calculations are done for both GLAO and NOAO cases in the aforementioned seeing conditions. In general, GLAO provides a rough $\sim 0.3 - 0.5$ magnitude improvement in standard NIR broad-band filters compared to NOAO under most seeing cases.

3.2 Throughput

The key throughputs for consideration are that of the atmosphere, primary+secondary mirrors, the GLAO system and that of the detector and filters. The values are given in Table 2 for the JHKs bands. The atmospheric transmission was determined from the Gemini transmission spectrum as shown in Fig 1. The primary and secondary mirror transmissions were directly measured at the telescope. The GLAO system transmission is set to the maximum 100% as no additional optics will be required in the science path for the GLAO wavefront sensor. Finally, the instrument and filter throughput is tentatively set to a constant value of 0.45 (best case target) at all wavelengths.

Filter	Wav	Airmass	GLAO _G	GLAO _M	GLAO _B	NOAO _G	NOAO _M	NOAO _B
Y	1	1	0.4255	0.5599	0.7557	0.5479	0.6871	0.8803
J1	1.2	1	0.3892	0.5197	0.7103	0.5266	0.6618	0.8561
J2	1.4	1	0.3569	0.4831	0.6701	0.5076	0.639	0.8192
H1	1.6	1	0.3341	0.4496	0.6343	0.5007	0.6284	0.8045
H2	1.8	1	0.3171	0.4249	0.6021	0.4882	0.6183	0.7822
Ks	2	1	0.3039	0.4035	0.5728	0.4757	0.5954	0.7622
K1	2.2	1	0.2953	0.3863	0.5467	0.4666	0.5858	0.7446
K2	2.4	1	0.2904	0.3729	0.5264	0.4591	0.5731	0.7327

Filter	Wav	Airmass	GLAO _G	GLAO _M	GLAO _B	NOAO _G	NOAO _M	NOAO _B
Y	1	1.5	0.57	0.73	0.96	0.7	0.87	1.1
J1	1.2	1.5	0.53	0.68	0.91	0.67	0.84	1.05
J2	1.4	1.5	0.49	0.65	0.87	0.65	0.82	1.02
H1	1.6	1.5	0.46	0.61	0.83	0.64	0.8	1
H2	1.8	1.5	0.43	0.57	0.79	0.62	0.77	0.97
Ks	2	1.5	0.41	0.55	0.76	0.61	0.76	0.95
K1	2.2	1.5	0.39	0.52	0.73	0.59	0.74	0.93
K2	2.4	1.5	0.38	0.5	0.7	0.58	0.72	0.91

Filter	Wav	Airmass	GLAO _G	GLAO _M	GLAO _B	NOAO _G	NOAO _M	NOAO _B
Y	1	2	0.688	0.8726	1.1225	0.8195	1.0134	1.246
J1	1.2	2	0.6433	0.8231	1.0724	0.7902	0.9752	1.2083
J2	1.4	2	0.6038	0.7785	1.0256	0.7615	0.9425	1.1745
H1	1.6	2	0.5672	0.7379	0.9842	0.7475	0.9241	1.151
H2	1.8	2	0.5353	0.7017	0.9447	0.7266	0.8994	1.1236
Ks	2	2	0.5081	0.6693	0.9097	0.708	0.8786	1.1018
K1	2.2	2	0.4841	0.64	0.8769	0.6957	0.8599	1.0765
K2	2.4	2	0.4636	0.6145	0.8463	0.6804	0.8433	1.0561

Table 1: The 50% Encircled Energy (EE_{50}) diameter in arcseconds of the simulated PSF for good (25%), moderate (50%) and bad (75%) seeing cases with GLAO and NOAO (natural seeing). From top to bottom, the tables give EE_{50} values for airmass of 1.0, 1.5 and 2.0.

Throughput	J	H	Ks
Atmosphere	0.98	0.98	0.92
Primary Mirror	0.95	0.95	0.95
Secondary Mirror	0.97	0.98	0.98
GLAO	1	1	1
Instrument+Filter	0.45	0.45	0.45

Table 2: The throughputs in the J, H and Ks bands for the atmosphere, telescope primary mirror, secondary mirror, GLAO system and the instrument+filter combination.

3.3 Sensitivity

The Signal-to-Noise equation is as follows:

$$S/N = \frac{0.5\lambda f_\lambda At_{exp}\eta_{tot}(\lambda)\Delta\lambda/hc}{\sqrt{N_{obj} + I_{BG}t_{exp}(\pi D_{ee50}^2/4) + (N_r\sqrt{\pi(D_{ee50}/ps)^2/4})^2}}, \quad (3)$$

where f_λ is the total flux density in $erg/sec/cm^2/\text{\AA}$, A is the telescope collection area in cm^2 - defined as $A = \pi D_p^2(1 - v_c^2)/4$, D_p is the effective diameter of the telescope primary mirror, t_{exp} is the exposure time in seconds, η_{tot} is the total throughput from all sources combined, N_{obj} is the object photon count, I_{BG} is the total background count in $photons/sec/arcsec^2$ from equation 1, D_{ee50} is the diameter of the 50% encircled energy as shown in table 1, N_r is the detector readout noise in e^-/rms and ps is the pixel scale.

Re-arranging equation 3 for the flux f_λ , we get:

$$f_\lambda = \frac{2\frac{S}{N}\frac{hc}{\Delta\lambda}\sqrt{N_{obj} + I_{BG}t_{exp}(\pi D_{ee50}^2/4) + (N_r\sqrt{\pi(D_{ee50}/ps)^2/4})^2}}{At_{exp}\eta_{tot}(\lambda)}, \quad (4)$$

The limiting magnitude is then simply calculated using the following equation:

$$M = -2.5\log f_\lambda - 5\log(\lambda) - 2.408 \quad (5)$$

Assuming a S/N of 5 and an exposure time of 1 hour, we calculate the 5σ limiting magnitudes in the YJHKs filters from equation 5. Given that for long exposures the dominant noise is the background noise (I_{BG}), the contribution from the object (N_{obj}) is assumed to be negligible. Figures 2 and 3 show sensitivities in MOIRCS broad-band and narrow-band filters using the background models and parameters defined above for WFI at Cassegrain. Figure 4 shows sensitivities in SWIMS medium-band filters. The sensitivities are calculated for three different combinations of airmass/water vapor - 1.0/1.0mm, 1.5/1.6mm, 2.0/3.0mm.

3.4 Sky Background vs. Telescope Background vs. Moon Background vs. Read Noise

As discussed earlier, the noise in the instrument is a combination of the sky background, the telescope thermal background, the moon background and the instrument read noise. We performed a cursory analysis of the background levels from each source through a number of broad, medium and narrow-band filters to see which source dominates the background level under differing circumstances and if any observations are read-noise limited under very short exposures. In Fig. 5 we plot the % of total the background count taken up by each source with increasing (short 1-30s) exposures under a variety of filters. In general, the read noise is never the dominant source in broad-band and medium-band observations even for very short exposures - at most the observations may be read noise limited (particularly in the Y-band and some medium K-band filters) for 1-2 seconds. For these filters the sky background dominates in most cases - though in the K-band region (particularly in the longest wavelength end), the telescope thermal background can become the dominant source of noise. The moon background is negligible at all wavelengths longer than the Y-band, even in which it appears at a nominal percentage of the overall background level.

Narrow-band observations can be read noise limited between 5-15 second exposures (based on filter), after which the contribution from read noise sharply drops off in comparison to the sky/telescope background. The specific exception once again is the NB119 filter in the Y-band, where the exposures can be read noise limited in excess of 30 seconds. As such for the vast majority of observations, the read noise will not need to be a significant concern in calculating limiting magnitudes except if NB observations are being conducted for very short exposure times.

3.5 Sensitivity Calculator

The Sensitivity Calculator is available at the following link, along with instructions on how to run. It allows for most parameters discussed in this report to be adjusted freely through a user-friendly interface. The following parameters can be changed in order to calculate the sensitivity estimates, with default values given in brackets:

- Exposure time (1 hour)
- Signal-to-noise ratio (5)
- AO: GLAO or NOAO (GLAO)
- Read noise ($16 e^-$ rms)
- Pixel scale ($0.1''/pix$)
- Airmass and water vapor levels for the sky background model ($am = 1.0, wv = 1.0\text{mm}$)
- Telescope background temperature (273K)
- Filters: All MOIRCS and SWIMS broad, medium and narrow-band filters are available. Custom filters can be used by inputting the filter central wavelengths and widths, as well as the transmission.

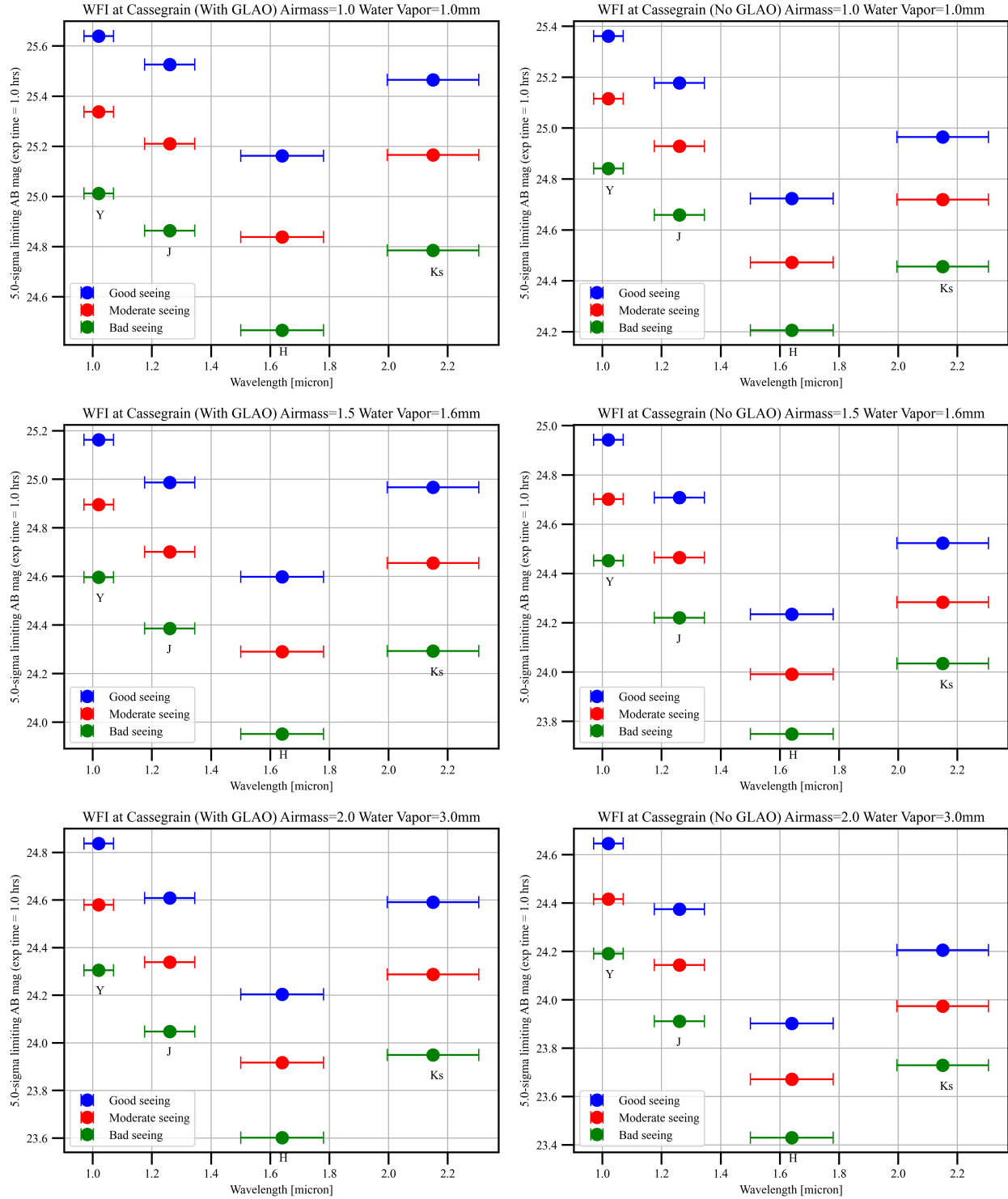


Figure 2: The WFI 5σ limiting magnitudes for 1 hour exposures in MOIRCS broad-band filters with GLAO (left) and NOAO (right). The sensitivities are calculated for three different seeing cases - good (25%), moderate (50%) and bad (75%). The plots from top to bottom show sensitivities for different combinations of airmass (1.0, 1.5, 2.0) and water vapor (1.0, 1.6, 3.0mm) respectively.

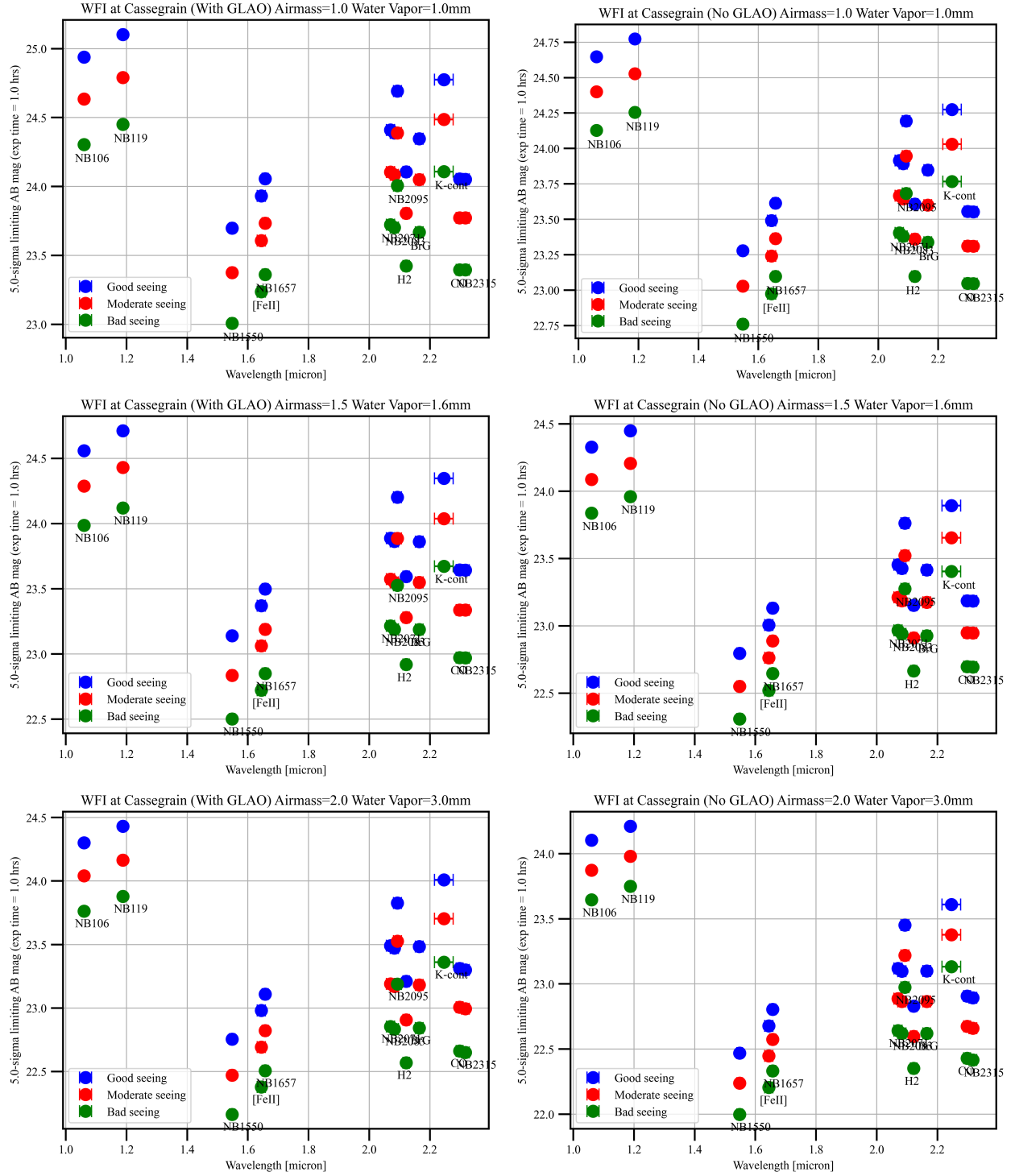


Figure 3: The WFI 5σ limiting magnitudes for 1 hour exposures in MOIRCS narrow-band filters with GLAO (left) and NOAO (right). The sensitivities are calculated for three different seeing cases - good (25%), moderate (50%) and bad (75%). The plots from top to bottom show sensitivities for different combinations of airmass (1.0, 1.5, 2.0) and water vapor (1.0, 1.6, 3.0mm) respectively.

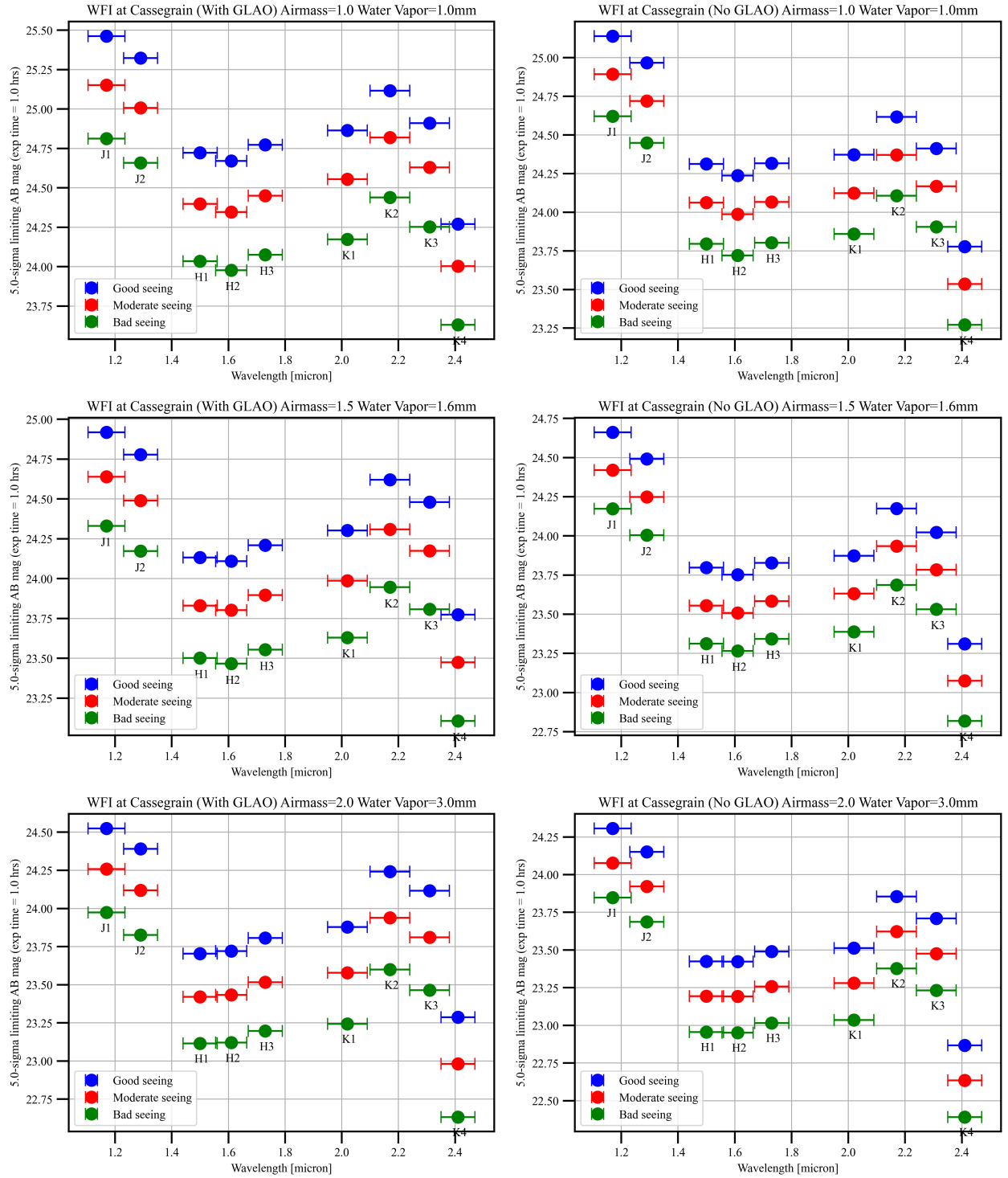


Figure 4: The WFI 5σ limiting magnitudes for 1 hour exposures in SWIMS (J1, J2, H1, H2, H3, K1, K2) and MOIRCS (K3, K4) medium-band filters with GLAO (left) and NOAO (right). The sensitivities are calculated for three different seeing cases - good (25%), moderate (50%) and bad (75%). The plots from top to bottom show sensitivities for different combinations of airmass (1.0, 1.5, 2.0) and water vapor (1.0, 1.6, 3.0mm) respectively.

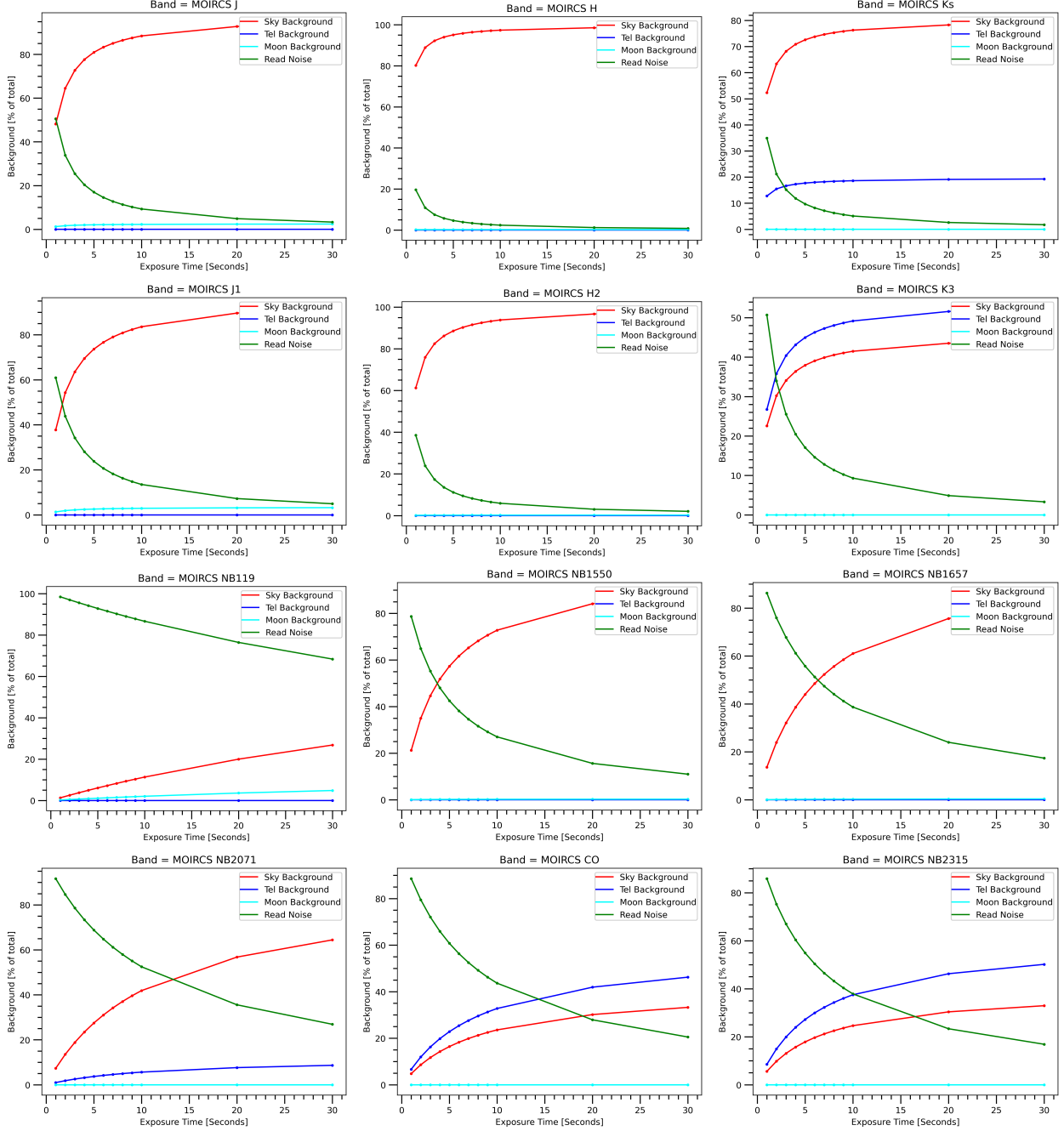


Figure 5: The background levels (as a % of total) from the sky, telescope, moon and read noise for short exposures. The models assume airmass=1.0, water vapor=1.0 mm and GLAO. Filters shown are a combination of MOIRCS broad-band (J, H, Ks), SWIMS medium-band (J1, H2, K3) and MOIRCS narrow-band (NB119, NB1550, NB1657, NB2071, CO, NB2315).